Journal of Thermal Analysis and Calorimetry, Vol. 68 (2002) 865–875

A COMPUTER PROGRAM BASED ON FINITE DIFFERENCE METHOD FOR STUDYING THERMAL INITIATION OF EXPLOSIVES

M. Sućeska

Brodarski Institut, Marine Research and Special Technologies, Av. V. Holjevca 20, 10000 Zagreb, Croatia

(Received October 10, 2001; in revised form November 14, 2001)

Abstract

The thermal decomposition of an explosive material is accompanied by generation of a certain amount of heat and, under certain conditions, can lead to the well-known phenomena of self-ignition. Therefore, it is of great importance to predict whether or not an explosive material will ignite under given conditions (specimen mass and shape, surrounding temperature, etc.).

An own computer program named THERMEX, for studying thermal ignition phenomena, is discussed in this paper. The program uses the finite difference method to describe the reactive heat conduction phenomena in infinite slab, cylindrical, and spherical geometry of explosive materials.

The analysis of the stability requirements of the finite difference method applied in the program is carried out. The program is tested by the comparison of calculated results with the results of calculation by other authors. Reasonable agreement was found under identical computational conditions.

Keywords: explosives, finite difference method, reactive heat conduction, self-ignition, thermal explosion theory, thermal initiation

Introduction

If the specimen of an explosive is heated, and if it decomposes according to the zero-order kinetic law, then the specimen heat balance can be described by the following equation [1]:

$$\rho c \frac{\partial T}{\partial t} = \lambda \nabla^2 T + \rho Q A e^{(-E/RT)} \tag{1}$$

where T is temperature (K); t – time (s); c – specific heat capacity (J kg^{-1} K^{-1}); ρ – density (kg m^{-3}); λ – thermal conductivity (W m^{-1} K^{-1}); ∇^2 – Laplacian operator; Q – heat of decomposition (J kg^{-1}); E – activation energy (J mol^{-1}); A – pre-exponential factor (s^{-1}), and R – universal gas constant (J mol^{-1} K^{-1}).

The left-hand side of Eq. (1) gives the rate of the heat build-up in the specimen of an explosive; the first term in the right-hand side is the rate of heat loss into the sur-

1418–2874/2002/ $ 5.00

Akadémiai Kiadó, Budapest
Kluwer Academic Publishers, Dordrecht

roundings; while the last right-hand term is the rate of heat generation due to exothermic reactions obeying the zero-order kinetic law.

The thermal ignition of explosives in ammunition is always the problem for concern. This is the reason why the explosive community is permanently searching for an efficient method for solving reactive heat conduction problem in explosives. The analytical solution to the heat conduction problem in the absence of chemical reactions, the so-called non-reactive heat conduction, is relatively easy to deduce, however, the analytical solution of the heat conduction equation with chemical reactions, the socalled reactive heat conduction, is out of question. Thus, the approximate techniques and the numerical methods are the most frequently subjects of investigation in this field.

Different simplifications to Eq. (1) have been proposed in order to calculate the critical conditions of self-ignition. Semenov [2], for example, allowed the temperature to be uniform through a sample, and reactions to follow the zero-order kinetic law. He was than able to compare the heat generation and the heat loss rates, and to derive the critical conditions of self-ignition. Frank-Kamanetskii [3]tried to find steady state solution of Eq. (1) in the case of the zero-order kinetic law, but without assuming the temperature to be spatially uniform through a specimen, i.e. applying the heat transport by convection.

To obtain the time-dependent solution of the heat of equation, different numerical techniques were proposed. Zinn and Mader used a numerical method based on a Fourier series spatial representation of solutions to obtain ignition times for slabs, cylinders, and spheres of the explosive material [1, 6]. Merzhanov and Abramov [4] were the first that applied the finite difference method to solve the heat conduction equation with the zero-order kinetic reaction model. Anderson developed the finite difference code for the one-dimensional heat conduction, based on the zero-order kinetic model and the Crank-Nicolson method. This code treats the problems of layered media in slabs, cylindrical, or spherical geometry, and incorporates temperature dependent thermal properties and phase transitions [7].

Since the thermal decomposition model plays a crucial role in each numerical method, some authors have tried to incorporate more complex kinetic model into computer codes based on the finite difference method. For example, Isler used successfully the power law kinetic model ($d\alpha/dt=k\alpha^n$) to describe the thermal ignition of a nitrocellulose propellant [5, 8]. McGuire and Tarver used 2-3 steps chemical decomposition models, deduced from available kinetic data for some explosives, and incorporated them to a thermal conduction code based on the finite difference method, obtaining a good agreement with experimental results [9].

Generally, one can note that the finite difference method is widely used to describe the reactive heat conduction phenomena in explosives, in connection with different kinetic models used to describe the thermal decomposition of explosives.

Some problems connected with the application of the finite difference method, such as stability and truncation requirements, ignition and boundary conditions, correct kinetic model, temperature-dependent thermal properties of an explosive, etc., are still subjects of improvements. This paper discusses some of these problems.

The numerical technique applied in THERMEX

In the special case of infinite long cylinders, infinite slabs, and sphere, the Laplacian operator (∇^2) in the general heat conduction equation (Eq. (1)) reduces in one dimension [6]:

$$\nabla^2 = \lambda\left(\frac{\partial^2}{\partial r^2} + \frac{m}{r}\frac{\partial}{\partial r}\right) \tag{2}$$

where r is radius of cylinder (or sphere). The integer m has a value 0 for slabs, 1 for cylinders, and 2 for spheres. In the case of an infinite slab r replaces by slab thickness (x). Thus, for example, Eq. (1) for an infinitely long cylinder will have the form:

$$\rho c\frac{\partial T}{\partial t} = \lambda\left(\frac{\partial^2 T}{\partial r^2} + \frac{1}{r}\frac{\partial T}{\partial r}\right) + \rho Q A e^{-E/RT} \tag{3}$$

The time dependent solution of Eq. (3) can be obtained by applying the finite difference method, i.e. by approximating partial derivatives with finite differences. The finite difference scheme of an infinitely long cylinder whose time-dependent temperature field we wish to compute from an initial temperature distribution, surrounding temperature, and boundary conditions may be represented by Fig. 1.

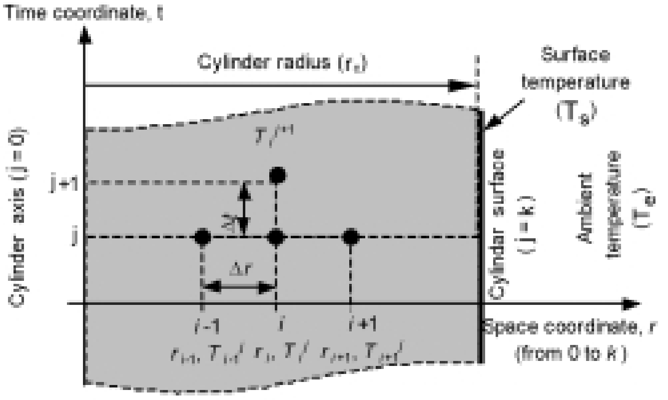

Fig. 1 The finite difference scheme of an infinitely long cylinder

The radius of an infinitely long cylinder (r_c) is divided into k cells, thickness of which is Δr ($\Delta r = r_c/k$). The initial temperature (at t=0, i.e. j=0, where j is a time index) is specified at individual mesh points ($T_{0,i}^{j=0}$, i=0 to k–1, where i is a space index), while the temperature at the cylinder surface (T_s^j) is specified by the boundary conditions (Eqs (11) and (12)).

For the case of an infinitely long cylinder the space derivatives in Eq. (3), in a time *j*, may be approximated by the following finite differences [7]:

$$\left(\frac{\partial^2 T}{\partial r^2}+\frac{1}{r}\frac{\partial T}{\partial r}\right)=\left(\frac{T_{i+1}^j+T_{i-1}^j-2T_i^j}{(\Delta r^2)}+\frac{1}{r}\frac{T_{i+1}^j-T_i^j}{\Delta r}\right) \tag{4}$$

For the case of spheres and infinite slabs the space derivatives will be [7]:

$$\left(\frac{\partial^2 T}{\partial r^2}+\frac{2}{r}\frac{\partial T}{\partial r}\right)=\left(\frac{T_{i+1}^j+T_{i-1}^j-2T_i^j}{(\Delta r^2)}+\frac{2}{r}\frac{T_{i+1}^j-T_i^j}{\Delta r}\right) \tag{5}$$

$$\left(\frac{\partial^2 T}{\partial x^2}\right)=\left(\frac{T_{i+1}^j+T_{i-1}^j-2T_i^j}{(\Delta x^2)}\right) \tag{6}$$

The time derivative in Eq. (3) may be replaced by its simplest finite difference approximation [7]:

$$\left(\frac{\partial T}{\partial t}\right)=\frac{T_i^{j+1}-T_i^j}{\Delta t} \tag{7}$$

where Δt is a time increment.

By replacing the space and time derivatives in Eq. (3) by the finite differences (Eqs (4)–(7)), the equation for the calculation of the temperature distribution along a space co-ordinate, at time t^{j+1}, can be derived. For example, in the case of an infinitely long cylinder this equation will be:

$$T_i^{j+1}=T_i^j+\frac{\lambda(\Delta t)}{c\rho}\left(\frac{T_{i+1}^j+T_{i-1}^j-2T_i^j}{(\Delta r^2)}+\frac{1}{r}\frac{T_{i+1}^j-T_i^j}{\Delta r}\right)+\frac{(\Delta t)}{c}QAe^{(-E/RT)} \tag{8}$$

It follows from the above equation that the temperature distribution along a cylinder radius at time t^{j+1} is evaluated from the temperature distribution at earlier time (t^j), where:

$$t^{j+1}=t^j+\Delta t \tag{9}$$

By an analogous way the equations for the calculation of the temperature distribution along a sphere radius or a slab thickness can be obtained from Eqs (5)–(7) and (3).

Initial and boundary conditions

In additions to the finite difference approximation to the reactive heat conduction equation, the approximations to the initial and boundary conditions should be included in order to calculate time-temperature distribution along a specimen space co-ordinate.

The initial conditions give an initial temperature distribution (at t=0) along a specimen co-ordinate. In the most usual way the initial conditions are given in the form:

$$T_i^{j=0} = T_{0,i}^{j=0} \text{ where } i=0, 1, 2, 3 \ldots k-1 \tag{10}$$

The boundary conditions give the temperature at a specimen surface at any time (T_s^j). The simplest case is when the specimen surface temperature remains constant during the whole process. In this case the boundary conditions can be written in the form:

$$T_s^j = T_e = \text{const.} \tag{11}$$

where T_e is the surrounding temperature. However, in the case of convective heat transfer from an ambient fluid to a specimen surface, the boundary conditions are given by the following equation [7, 8]:

$$\begin{gathered} \varepsilon(T_s - T_e) = -\lambda\left(\frac{\partial T}{\partial r}\right)_s, \text{ i.e.} \\ \varepsilon(T_s - T_e) = -\lambda\frac{T_s - T_{k-1}}{\Delta r} \end{gathered} \tag{12}$$

where ε is the heat transfer coefficient (W m^{-2} K^{-1})

Results and discussion

On the basis of the numerical technique described above, the computer program named THERMEX was written. Having in mind that an explicate finite difference solution to the differential equations is often conditionally stable, and that the correct choice of space and time increments is of crucial importance to obtain accurate solutions, the first step in this work was to analyse the influence of time and space increments on the results of calculations.

As a test model hexogen (RDX) spheres 25.4 mm in diameter were used. The spheres, being initially at the temperature of 25°C, were subjected instantaneously to the surrounding temperatures higher than the critical ones – in the 180–260°C range. The same test model was used by Zinn and Mader [1, 6], and by Anderson [7] to study numerically the thermal ignition phenomena of RDX (Table 1).

The values of the kinetic and thermal parameters of RDX used in calculations are given below [1, 6, 10]:

ρ = 1.8 g cm^{-3} Q = 2093 J g^{-1}
E = 199 kJ mol^{-1} A = 3.16 10^{18} s^{-1}
c = 2.093 J K^{-1} g^{-1} λ = 0.293 W m^{-1} K^{-1}

The times to the thermal ignition at given surrounding temperature are calculated for several different space and time increments, applying the boundary conditions given by Eq. (11). As an example, the results of calculations for surrounding temperature of 240°C are shown in Fig. 2.

It is evident from Fig. 2 that times to ignition depend strongly on the values of space and time increments. For the small values of time increments, the time to ignition-time increment relationships is practically linear. The slopes and the intersections of individual time to ignition-time increment curves with Y axis depend on the space increment.

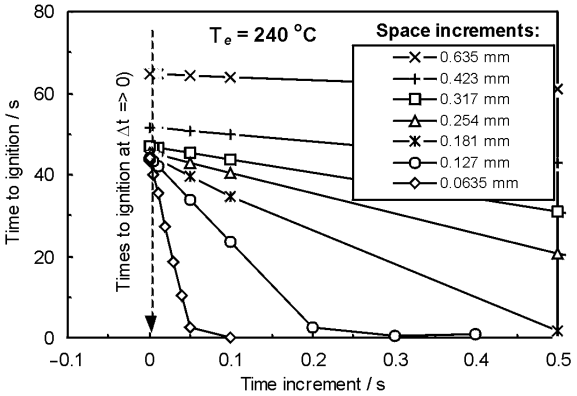

Fig. 2 The dependence of calculated times to ignition of RDX sphere on time increment for different space increments at surrounding temperature of 240°C

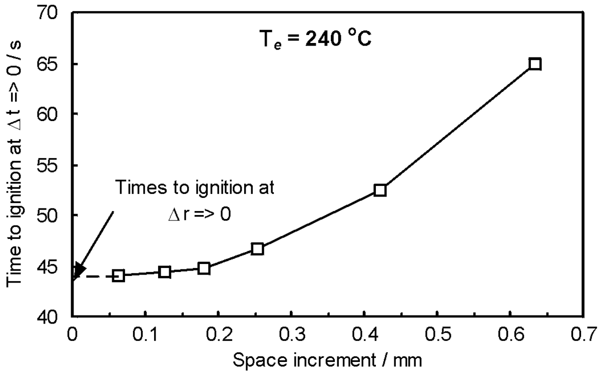

Fig. 3 The dependence of calculated times to ignition of RDX sphere on space increment at surrounding temperature of 240°C

By the linear extrapolation of the time to ignition-time increment data given in Fig. 2, the values of time to ignition corresponding to $\Delta t \to 0$ were derived for individual space increments. In this way the dependence of time to ignition at $\Delta t \to 0$ ($t_{e\,\Delta t \to 0}$) on space increment is obtained (Fig. 3).

By the extrapolation of the non-linear dependence times to ignition-space increment, given in Fig. 3, time to ignition at $\Delta r \to 0$ ($t_{e\,\Delta t \to 0,\,\Delta r \to 0}$) for specified surrounding temperature is obtained. The values of times to ignition for several surrounding temperatures, obtained by this procedure are given in Table 1, along with the values obtained by other authors.

It follows from Table 1 that the ignition times obtained in this way are in good agreement with Zinn and Mader and Anderson calculations. However, a normal way of the calculation of ignition times and the space and time temperature profiles inside a specimen is to use sufficiently small time and space increments. If time and space increments are not sufficiently small, small errors in data may generate a large total error. Thus, the correct choice of space and time increments is of crucial importance.

Table 1 Times to ignition for RDX spheres calculated by different authors

Surrounding temperature/°C	Time to ignition/s			
	Zinn and Mader [1, 6]	Anderson, code TEPLO [7]	Anderson, code TEPLO [7]*	This work (code THERMEX)
180	1000	1030	1200	1051.8
200	420	458	593	466.9
220	120	162	183	166.1
240	33	42.9	43.8	44.0
260	10.5	10.1	10.0	10.3

*Time to ignition is calculated taking temperature-dependent heat capacity and taking the melting of RDX into account

The analysis carried out in this work has shown that, in order to obtain the times to ignition which do not differ more than 1% in respect to the times obtained by the extrapolation of data to $\Delta r \to 0$, the space increment should be less than 0.06 mm for the 260°C surrounding temperature; less than 0.15 mm for the 240°C surrounding temperature, etc. (Fig. 4).

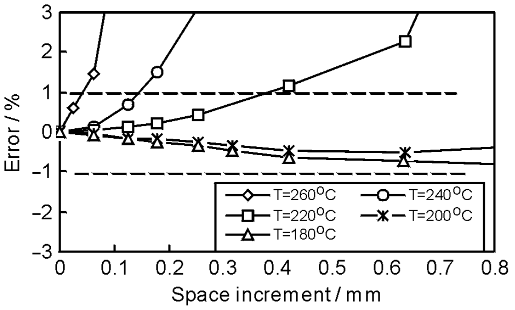

Fig. 4 The error in calculated values of times to ignition *vs*. space increment for several surrounding temperatures (where: error=$(t_e - t_{e\,\Delta t\to 0,\,\Delta r\to 0})100/t_{e\,\Delta t\to 0,\,\Delta r\to 0}$)

It is obvious from Fig. 4 that, in order to obtain a high level of accuracy (e.g. the error in the calculation of the times to ignition less than 1%), the space increment has to be very small – from some tenth of microns to some hundreds of microns, depending on the surrounding temperature.

Further analysis has shown that the time increment, which enables the times to ignition to be calculated with a small error, may be chosen on the basis of the stability criterion given by the equation [7]:

$$\frac{\lambda}{\rho c}\frac{\Delta t}{(\Delta r)^2}<f_s \tag{13}$$

According to Richtmyer's results (cited in [7]) the finite difference method is stable if $f_s<0.5$. The results of the presented work have shown that, in order to obtain a ignition times which differ less than 1% in the respect to ignition times obtained by the extrapolation to $\Delta t\rightarrow 0$, the value of f_s should be less than 0.01 (Fig. 5). It should be noted that almost the same value of f_s was obtained for all surrounding temperatures in the 180–260°C range.

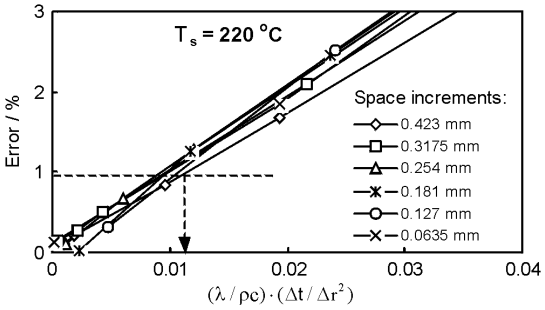

Fig. 5 The error in values of calculated ignition times *vs*. value of $(\lambda/\rho c)(\Delta t/\Delta r^2)$

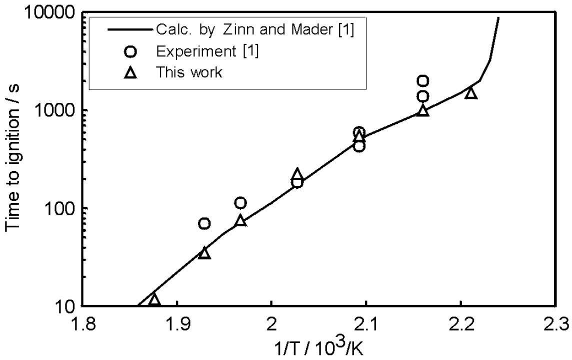

Fig. 6 The comparison of experimentally obtained and calculated ignition times for an RDX cylinder 25.4 mm in diameter

On the basis of this criterion, it follows that, at the surrounding temperature of 260°C and the space increment of 0.06 mm, the time step should be less than 0.0001 s in order to obtain the ignition times that differ less than 1% in respect to the ignition times obtained by the extrapolation to $\Delta t \to 0$; for the surrounding temperature of 220°C the space increment should be less than 0.4 mm, and the corresponding time increment should be about 0.02 s, etc.

Times to ignition are also calculated for a 25.4-mm diameter RDX cylinder, and compared with the experimentally obtained values. The results of the comparison are shown in Fig. 6. A reasonable good agreement was found between the experimentally obtained and calculated ignition times, as well as between the results of calculation in this work and those obtained by Zinn and Mader [1].

Space- and time-temperature profiles

Although the time to ignition and the critical temperature are the essential parameters for the prediction of self-ignition possibility of an explosive specimen, we are usually interested in having details of the heat flow, i.e. to have the temperature-time profile at a given position within a specimen, and the temperature-radius profile at a given time.

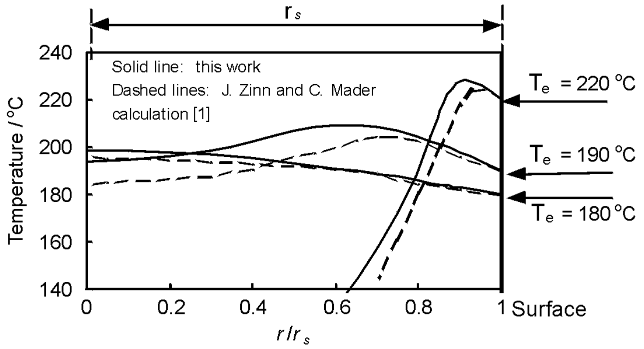

Fig. 7 The calculated temperature-radius profiles for the times near the end of induction period ($t=t_e0.95$) for RDX sphere 25.4 mm in diameter, being initially at 25°C

It is known that the time to ignition decreases with the surrounding temperature increase (Table 1), as well as that the ignition of the specimen occurs at a position closer to the specimen surface with the increase of the surrounding temperature. The last is visible from Fig. 7, which shows the spatial distribution of the temperature for RDX spheres subjected to the several different surrounding temperatures.

For the surrounding temperature of 220°C the ignition occurs at the position $r/r_s \approx 0.95$, while at the same time the centre of sphere remains relatively cool during the whole induction period. For low surrounding temperatures, e.g. 180°C, the ignition occurs at the centre of sphere. At the same time the surface of the sphere remains at the surrounding temperature. The results of the calculation are in agreement with the results of the calculation by Zinn and Mader [1].

The above mentioned is also visible from Fig. 8, showing the time-temperature distribution at two locations within the RDX sphere subjected to 190°C surrounding

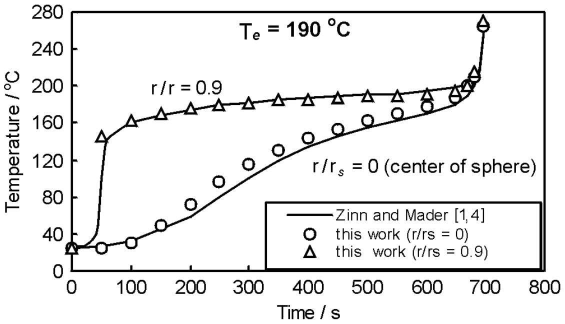

Fig. 8 The calculated temperature-time profiles at two locations inside a 25.4 mm diameter sphere of RDX subjected to the 190°C surrounding temperature

temperature. At the location r/r_s≈0.9 the temperature increases relatively quickly, while at the centre of sphere the temperature reaches the same value only at the end of the induction period. The results of calculation are again in the reasonable agreement with the results of calculation by Zinn and Mader [1].

Conclusions

The presented numerical model for studying the initiation phenomena of explosives, based on the finite difference method, can be used to predict the time to ignition, and critical temperature, as well as to obtain the temperature-time, and the temperature-space co-ordinate profiles of an explosive material specimen.

It is shown that the accuracy of the solution is greatly affected by the values of the space and time increments. The correct value of the space increments for a given surrounding temperature may be determined by preliminary calculations (Figs 2 and 3), while the correct value of time increments for a given space increment may be determined on the basis of the stability criterion $(\lambda/\rho c)(\Delta t/\Delta r^2)<0.01$.

The results of the calculations for the selected test model are in reasonable agreement with the results of calculation by some other authors, making thus THERMEX program a useful tool in studying the thermal initiation phenomena.

References

1 J. Zinn and C. L. Mader, J. Appl. Phys., 31 (1960) 323.
2 N. N. Semenov, Z. Phys., 42 (1928) 571.
3 D. A. Frank-Kamentskii, Acta Physiochim, U.R.S.S., 10 (1939) 365.
4 A. G. Merzhanov and V. G. Abramov, Propellants and Explosives, 6 (1981) 130.
5 J. Isler and D. Kayser, Correlation Between Kinetic Properties and Self-Ignition of Nitrocellulose, 6th Symp. Chem. Probl. Connected Stab. Explos., Kungalav, Sweden 1982, p. 217.

6 C. L. Mader, Numerical Modeling of Explosives and Propellants, CRC Press, Boca Raton 1998, p. 136.
7 C. A. Anderson, TEPLO – A Heat Conduction Code for Studying Thermal Explosion in Laminar Composites, Report LA-4511, Los Alamos Scientific Laboratory, Los Alamos 1970.
8 J. Isler, Propellants, Explos. Pyrotechn., 11 (1986) 40.
9 R. R. McGuire and C. M. Tarver, Chemical Decomposition Models for Thermal Explosion of Confined HMX, RDX, and TNT Explosives, Report UCRL-84986, Lawrence Livermore Laboratory, Livermore 1981.
10 J. F. Baytos, Specific Heat and Thermal Conductivity of Explosives, Mixtures, and Plastic-Bonded Explosives Determined Experimentally, Report LA-8034-MS, Los Alamos Scientific Laboratory, Los Alamos 1979.